doi:10.2533/chimia.2023.417 Chimia 77 (2023) 417–423 

# Late Microaerobic Growth for Efficient Production of Human Cytochrome P450 3A4 in *E. coli*

Luca Marchetti, Matteo Planchestainer, Sven Panke, and Martin Held*

*Abstract:* Detailed preclinical characterization of metabolites formed *in vivo* from candidate drug substances is mandatory prior to the initiation of clinical trials. Therefore, inexpensive, and efficient methods for drug metabolite synthesis are of great importance for rapid advancement of the drug development process. A large fraction of small molecule drugs is modified by monooxygenase cytochrome P450 3A4 (CYP3A4) produced in the human liver and intestine. Therefore, this enzyme is frequently employed to catalyze metabolite synthesis *in vitro*, making CYP3A4 availability a critical requirement in early drug development. Unfortunately, the recombinant production of this enzyme in microbial hosts is notoriously difficult. Maintaining low oxygen transfer rates and the use of rich media for host cultivation are required for CYP3A4 production. However, detailed studies on the relationship between oxygen supply and P450 CYP3A4 space-time yields are missing. We describe an improved biotechnological process for the heterologous expression of CYP3A4 together with its redox partner, human cytochrome P450 reductase (*h*CPR), in *Escherichia coli*. Enzyme production was most efficient under so-called 'late microaerobic' growth conditions, in which the cells have just not yet switched to anaerobic metabolism. This regime is characterized by a limited oxygen supply leading to oxygen concentrations in the liquid phase that are far below the detection limit of standard oxygen electrodes. Furthermore, feeding the carbon source glycerol as well as controlling cellular acetate formation improved process productivity. The presented protocol resulted in the formation of functional recombinant CYP3A4 at concentrations up to 680 nmol $L^{-1}$.

**Keywords**: Biocatalysis · Cytochrome P450 · Drug development · Fermentation

***Luca Marchetti*** studied Interdisciplinary Sciences (BSc) and Biotechnology (MSc) at ETH Zurich (CH). He worked on enzyme engineering in the research groups of Profs. Hilvert (ETHZ) and Arnold (Caltech, USA) as well as on antibody engineering in the group of Prof. Reddy (ETHZ). For his Master thesis, he worked on the optimization of cytochrome P450 production with Dr. Held. After graduating, he interned at Securecell AG (CH), working on bioprocess automation and software validation, before returning to ETHZ to start a PhD in immuno-oncology with Prof. Reddy.

***Matteo Planchestainer*** studied Biotechnology at the University of Trento (BSc) and Industrial Biotechnology (MSc) at the University of Bologna in Italy. After graduating, he moved to the University College Dublin, (IE) and the University of Nottingham (UK) to complete a PhD in biocatalysis with Prof. Paradisi. He then spent two years as a postdoc at the University of Bern in the group of Prof. Albrecht, developing artificial metalloenzymes. In 2020, he joined the group of Prof. Panke at ETH Zurich as part of an interdisciplinary team working on bioprocesses for the production of valuable chemicals.

***Sven Panke*** studied Biotechnology at the Technical University of Braunschweig with Ken Timmis and worked as an undergraduate fellow for a year with Victor de Lorenzo at the Centro Nacional de Biologia before obtaining his doctoral degree from ETHZ in 1999 while working with Bernard Witholt. After that, he worked for 2 years for DSM Fine Chemicals and then joined ETH Zurich as an assistant professor for Bioprocess Engineering. Since 2017, he is a full professor at the Department of Biosystems Science and Engineering of ETHZ. His research interests are bioprocess and biocatalyst development and synthetic biology.

***Martin Held*** studied technical biology at the University of Stuttgart and did his PhD at the Institute of Biotechnology of the ETH Zurich in the field of microbially catalyzed fine chemical synthesis under the supervision of Bernard Witholt. In 2002, he joined the group of Prof. Panke at ETH Zurich, where he is working on the development of bioprocesses and catalysts for the biocatalytic synthesis of high-value-added chemicals, API intermediates, vitamins, and drug substances.

## 1. Introduction

The development of new drugs is a long, expensive, and challenging endeavour taking on average 10–15 years from the target-to-hit stage at costs of around $1.5 billion.[1,2] Gaining a thorough understanding of drug candidate metabolites formed in humans, and their contribution to the pharmacodynamics, pharmacokinetics, toxicity, and potential for causing off-target effects, is an essential part of the preclinical characterization stage.[3] Hence, robust methods for the preparative synthesis of drug metabolites are key. Because the synthesis of phase I hydroxylates of small molecules through organic chemistry methodologies is often complicated and laborious, biotransformation is routinely employed as an alternative synthesis strategy, and human cytochrome P450 (CYP) monooxygenases are of exceptional importance.[3,4]

### 1.1 *Cytochrome P450 Monooxygenases*

In humans, approximately 57 different CYPs are responsible for catalyzing the vast majority of phase I drug metabolism reactions.[5] Phase I reactions, comprising reduction, hydrolysis or hydroxylation, can convert drugs into inactive metabolites or turn prodrugs into active substances which cause or contribute to the

*Correspondence: Dr. M. Held, E-mail: martin.held@bsse.ethz.ch
1BPL, D-BSSE, ETH Zurich, Mattenstr. 26, Basel, CH-4058

desired pharmacological effects. However, phase I reaction products may also mediate unwanted side effects.[1] A single member of the CYP family, human cytochrome P450 monooxygenase 3A4 (CYP3A4) is involved in the metabolism of over 50% of all currently registered small molecule drugs.[6] Therefore, studying possible products of a candidate drug formed in CYP3A4-catalyzed reactions is a routine operation in drug development. Still, this routine operation remains a challenge as producing preparative amounts of CYP3A4 is difficult.[3,4]

### 1.2 *Recombinant CYP3A4 Synthesis*

CYPs occur naturally in almost every species, with *Escherichia coli* being a notable exception.[7] The absence of any interfering CYP activities makes *E. coli* a popular host for the recombinant production of human CYPs.[3] In fact, although a variety of expression systems have been developed, *E. coli* remains the preferred host for preparative scale (1–5 µmol) production because of low maintenance costs, ease of cultivation, and generally higher CYP expression levels compared to yeast or mammalian cell cultures.[8–10]

However, production of CYP3A4 in *E. coli* is only possible at peculiar cultivation conditions in complex media formulations (*i.e.* terrific broth).[11] Most laboratories still employ a protocol described by Gillam *et al.* in 1993.[9,12]. This empirically developed method is characterized by cultivation at low oxygen transfer rates under low energy input, typically realized through low shaking frequencies and high filling levels in non-baffled shake flasks exceeding the volumes recommended for cultivation of *E. coli* under aerobic conditions by far. Similar protocols have been developed for CYP3A4 production in bioreactors adjusting dissolved oxygen tensions (DOTs) to less than 1% (microaerobic conditions).[11,13]

Even though molecular oxygen is a substrate of CYP3A4, the enzyme is naturally mostly produced in oxygen-poor regions of the liver and intestine.[14] It is tempting to assume that low DOTs may stabilize CYP3A4, because at high oxygen concentrations, unproductive catalytic cycles can be triggered. In the course of these cycles (also known as 'uncoupling')[14] highly reactive oxygen species (ROS) are formed. ROS could then disrupt the active site of CYPs, for instance by oxidating the cysteine residue axially ligating the iron ion of the heme co-factor.[15] To this end, a low DOT may positively impact CYP3A4 stability.[13,16]

The propensity of CYP3A4 to be deactivated by oxygen, the need for N-terminal modification to ensure membrane anchoring and proper folding, together with the requirement of co-expression of human cytochrome P450 reductase (*h*CPR) required for its activity, complicate the production of functional CYP3A4 in prokaryotic host cells.[10,17] Intriguingly, the aeration regime for active CYP3A4 production has never been carefully evaluated for very low DOTs.

Apart from influencing CYP3A4 stability, the DOT also drastically affects the metabolic state of *E. coli*.[18] Pedraz *et al.*[19] performed a comprehensive study on the adaptation of facultatively aerobic organisms to anaerobic conditions and defined a 'late microaerobic' regime during which *E. coli* exhibits a hybrid respiratory/fermentative metabolism.[19] Following the terminology coined by Pedraz *et al.* (aerobic: 25% – 100% DOT; microaerobic: >0% – 25% DOT; late microaerobic: ~0% DOT; anaerobic: 0% DOT / no $O_2$ supply),[19] we will refer to processes that still feature a continuous supply of oxygen, yet show a DOT below the lower limit of detection of the usually applied oxygen probes as 'late microaerobic' from here on.

Because human CYP3A4 is apparently produced best at very low DOTs, we hypothesized that optimizing the oxygen supply rate in late microaerobic cultivation regimes could allow higher yields of active CYP3A4. As starting point, we used an *E. coli* JM109 strain recombinantly expressing both human CYP3A4 and *h*CPR[20] which is in use at different pharmaceutical companies.[3] So far, the CYP3A4 yields that were reached have been rather low compared to other CYPs (400–500 $nmol_{CYP3A4}$ $L^{-1}$ as compared to 1,500 nmol $L^{-1}$ for CYP2C8).[9,11,21,22] We show that through careful monitoring and regulation of the cultivation parameters (*i.e.* pH, DOT, nutrients, metabolites) in bioreactors a reliable protocol can be established that results in substantially higher yields.

## 2. Materials and Methods

### 2.1 *Chemicals*

If not stated differently, the chemicals used herein were purchased from Thermo Fisher Scientific and Sigma-Aldrich at the highest available purity. *N*-ethyl-1,8-naphtalinimide (NEN), the model substrate for hydroxylation by CYP3A4, was synthesized in-house according to published protocols (yield: 55%, purity >99% by HPLC).[23]

### 2.2 *Buffers & Media*

All buffers and media were prepared with double distilled water ($ddH_2O$).

*Media*: Luria-Bertani medium (LB): DifcoTM LB Broth (25 g $L^{-1}$); Terrific Broth (TB): yeast extract (24 g $L^{-1}$), tryptone (20 g $L^{-1}$), and glycerol (5 g $L^{-1}$) were autoclaved separately before adding sterile filtered potassium phosphate ($KH_2PO_4$/$K_2HPO_4$ 2.3 g $L^{-1}$/12.5 g $L^{-1}$) and trace element solution (1.5 mg $L^{-1}$ $MnCl_2$, 1.05 mg $L^{-1}$ $ZnSO_4$, 0.3 mg $L^{-1}$ $H_2BO_4$, 0.25 mg $L^{-1}$ $Na_2MoO_4$, 0.15 mg $L^{-1}$ $CuCl_2$, 0.84 mg $L^{-1}$ $Na_2EDTA$, 4.87 mg $L^{-1}$ $FeSO_4$, 4.12 mg $L^{-1}$ $CaCl_2$ in 1 mM HCl; final concentrations). Antibiotics were used at concentrations of 100 mg $L^{-1}$ (carbenicillin) and 34 mg $L^{-1}$ (chloramphenicol), respectively.

*Assay buffers*: i) Wash/CO-binding: 50 mM KPi, pH 7.0; ii) NEN hydroxylation: 100 mM KPi, pH 7.4; iii) cytochrome c reduction: 300 mM KPi, pH 7.7.

### 2.3 *Production Strain JM109$^{CYP3A4/hCPR}$*

The CYP3A4 production strain described herein was developed from *E. coli* JM109 (K-12 derived) cells transformed with the expression plasmids pB51 (pelB-*h*CPR/ompA-CYP3A4) for the expression of N-terminally modified *h*CPR and CYP3A4, and pB233 (cytochrome b5).[9,20] On these plasmids, gene expression is controlled by IPTG-inducible Ptac promotors (sequence details in the supplementary information).

### 2.4 *Bioreactor Cultivation*

Bioreactor cultivation was carried out in Infors HT Minifors (working volume 1 L) or Minifors-2 (working volume 0.7 L) tabletop fermenters without flow disruptor inserts, equipped with acid and base pumps (HCl/NaOH, 2 M) for pH control (pH probe Metler Toledo InPro3100i/SG/225). DOT was measured using a dissolved oxygen sensor (Hamilton OxyFerm CIP). Dissolved oxygen sensor two point-calibration was performed by sparging uninoculated complete cultivation media with $N_2$ for 30 min (200 rpm) and setting the sensor signal to 0%. The medium was then supplied with air (21% oxygen) for 30 min (1,000 rpm), before setting the sensor signal to 100%.

Seed cultures of 25 mL in TB were initiated with 1 mL of an 8 h LB pre-culture inoculated from glycerol stocks and cultivated at 30 °C. The seed cultures were typically grown into the early stationary phase ($OD_{600}$ of approx. 5 after 9 h). The reactors contained TB medium and were inoculated to an $OD_{600}$ of 0.1 from the seed cultures. Around 3 h after inoculation ($OD_{600}$ = 0.8), synthesis of CYP3A4 and *h*CPR was induced by adding IPTG to a final concentration of 0.1 mM. At the same time, 5-aminolevulinic acid (5-ALA; 1.0 mM final concentration) was added in order to provide sufficient substrate for heme synthesis. Unless stated otherwise, airflow and stirring speed were kept constant over the

entire fermentation time. The operation window characterized with respect to varying OTRs (see Table S1 in the Supplementary Information) was chosen from 0.42–3.6 vvm (air volumetric flow rate per unit volume of culture medium) and from 100–600 rpm (stirring speed). For sampling, ~10 mL of liquid culture were removed from the reactors, centrifuged (3,200 g, 10 min), washed once with KPi wash buffer and recentrifuged. After discarding the supernatant, the pellet was stored at –20 °C.

Fermentations in the Minifors-2 reactor allowed off-gas analysis, which was carried out with a BlueVary sensor (applikon® BIOTECHNOLOGY). Respiratory quotient (RQ = $[CO_2]_{produced}$/$[O_2]_{consumed}$) values were calculated according to Franzén *et al.*[24]

For fed-batch fermentation processes, a 10% (v/v) glycerol solution was supplied with a feeding pump regulated using the custom parameter function interface from the eve® software for the Minifors-2 bioreactor (see Supplementary Information). Because changes in culture volume $\Delta V$ (*i.e.,* through sampling, base- and carbon source feeding) were minimal, the influence of $\Delta V$ on the volumetric airflow (vvm) and therefore the OTR were neglected.

## 2.5 $k_La^{app}$ Estimation

To characterize different aeration regimes in bioreactors, apparent volumetric mass transfer coefficients ($k_La^{app}$) were measured in fully assembled but non-inoculated fermenters (sterilized TB, 30 °C, pH = 7) using the 'gassing-out' method.[25] The determined $k_La^{app}$ is not equal to the actual $k_La$ throughout cultivation, as this value is influenced by growth, accumulation of surface-active compounds, and changes in media composition. Rather $k_La^{app}$ served as a means to compare different fermentation conditions with regard to the oxygen supply rates. To prevent excessive foaming, two drops (~100 µL) of antifoaming agent (Antifoam-204 Merck KGaA) were added at the beginning of the process for both the $k_La$ estimation experiment as well as the corresponding cultivation process for CYP3A4 production, if deemed necessary (see Table S1).

## 2.6 Enzyme Quantification/Activity Assays

All enzyme quantifications and activity assays were carried out in crude cell lysates: frozen cells obtained under various cultivation conditions were thawed at room temperature (RT) and resuspended in CO-binding buffer to an $OD_{600}$ of approximately 25 corresponding to 9 g cell dry weight (CDW) $L^{-1}$ (1 $OD_{600}$ = 0.35 gCDW $L^{-1}$)[26]. Cells were lysed on ice using a BRANSON™ SONIFIER 250 cell disruptor with a tapered 3 mm microtip (2 min, duty cycle: 50%, output: 2).

### 2.6.1 Quantification of Functional CYP3A4

Functional CYP3A4 production was quantified by the method developed by Guengerich *et al*.[27] Briefly, we measured the abundance of the characteristic Enz-S-Fe(II)-CO complexes after exposure to carbon monoxide. Crude cell lysates were treated with 10 mM sodium dithionite ($Na_2S_2O_4$) and incubated for 1 min at RT. Absorbance spectra (400–500 nm) were recorded before and after bubbling pure carbon monoxide through the lysates (1 min, 1 gas bubble per second in a paraffin oil counter). The concentration of functional CYP3A4 was calculated using the molar extinction coefficient ε of the Enz-S-Fe(II)-CO complex at 450 nm using $\varepsilon_{450nm}$ = 91,000 $M^{-1}$ $cm^{-1}$ (d = 1 cm). Guengerich *et al.* recommend enzyme concentrations of 0.5–5 µM P450 for optimal performance of the assay, corresponding to 55–550 nmol $gCDW^{-1}$ when measured in lysates of samples at $OD_{600}$ = 25.[27] The detection limit was estimated to be at around 50 $nmol_{CYP3A4}$ $gCDW^{-1}$.

### 2.6.2 CYP3A4 Activity Assay

To assess the activity of CYP3A4 in cell lysates, we used the hydroxylation of *N*-ethyl-1,8-naphtalinimide (NEN) as described by Ning *et al*.[23] (Scheme S1). Crude cell lysates were diluted with reaction buffer to adjust a concentration of 50 nM CYP3A4. An aliquot of 4 µL of a 10 mM NADPH stock in 50 mM KPi buffer (final concentration: 200 µM) and 4 µL of a 2.5 mM NEN stock in DMSO (final concentration: 50 µM NEN, 2% DMSO) were added as substrates resulting in a final total assay volume of 200 µL. Hydroxylation of NEN was monitored by measuring the increase of the *N*-ethyl-4-hydroxy-1,8-naphtalinimide (NEHN) fluorescence signal ($\lambda_{ex}$ = 450 nm, $\lambda_{em}$ = 550 nm, gain = 110, TECAN infinite M1000 PRO). Product formation was quantified by relating fluorescence signals to calibration curves determined for the device (Fig. S1A).

Enzyme activity is reported in units U (1 $U_{NEN}$ = 1 µmol NENH generated in 1 min). Turnover frequency is reported in $nmol_{NEN}$ converted per min per $nmol_{CYP3A4}$ as measured by the CO-binding assay.

### 2.6.3 hCPR Activity Assay

*h*CPR activity was quantified by a NADPH-cytochrome c reduction assay, as described in Guengerich *et al*.[27] In this assay, cytochrome c (cyt c) acts as a surrogate electron-acceptor and is directly reduced by *h*CPR, changing its absorption spectrum. Lysates were diluted to densities between 7 and 10 mg CDW $L^{-1}$ in $KP_i$ buffer. An aliquot of 8 µL of a 1 mM stock of equine heart cyt c in 50 mM KPi buffer was added to the diluted lysates on ice (final concentration: 40 µM cyt c). The reaction was initiated by adding 2 µL of a 10 mM stock of NADPH in 50 mM KPi buffer (final concentration 100 µM NADPH) resulting in a final total volume of 200 µL. The reduction of cyt c was monitored by measuring the absorbance signal of reduced cyt c at 550 nm ($\varepsilon_{550nm}$ = 29,500 $M^{-1}cm^{-1}$).[28] The *h*CRP activities are reported in U (1 $U_{cyt\ c}$ = 1 µmol cytochrome c reduced in 1 min).

### 2.6.4 CYP3A4 and hCPR Stability Assay

The stability of CYP3A4 and *h*CPR over the course of a NEN conversion experiment was assessed with the NEN conversion assay. NEHN production upon the addition of 200 µM NADPH was determined by measuring absorbance at $\lambda_{abs}$ = 450 nm (d = 0.66 cm) and interpolating the corresponding NEHN concentration from an empirical NEHN-absorbance calibration curve for the device (Fig. S1B). The remaining NEN was then readjusted to a concentration of 50 µM by adding substrate from a 1 M stock together with another 200 µM of NADPH (volume change <1%) to the reaction mixture after 1 h and again after 2 h of total reaction time. NENH formation rates were determined *via* the slope of the absorbance signal *vs* time in the first 5 min after NADPH addition (Fig. S6A). *h*CPR activity was measured before each addition of the cofactor by subjecting 2 µL of the reaction mixture to a standard cytochrome c reduction assay.

### 2.6.5 Protein Analytics

Proteins were analyzed by SDS-PAGE.[29] The cells were resuspended in wash buffer to an $OD_{600}$ = 5 (1.75 gCDW $L^{-1}$) and incubated in Laemmli Buffer at 99 °C for 5 min. An aliquot of 15 µL of the mixture was then loaded onto Invitrogen BoltTM 4–12% Bis-Tris Plus gels. Protein separation was achieved by gel electrophoresis (165 V) after 35 min.

For unequivocal protein identification, we used Western Blotting (WB): Proteins separated by SDS-PAGE were transferred onto PVDF WB Membranes from Roche Diagnostics GmbH using a BIO-RAD Mini-PROTEAN® 3 Cell device at 250 mA for 45 min. The membranes were washed in $ddH_2O$ and blocked with 5% non-fat dry milk powder in 1× Tris-buffered saline (20 mM Tris, 150 mM NaCl in $ddH_2O$) supplemented with 0.15% Tween 20 (TBST) for 1 h at RT. The primary antibody CYP3A4 mAB (3H8) from Invitrogen was diluted 1:1,000 in milk and used for staining of the membranes overnight at 4 °C. The membranes were washed with TBST before being stained once with a 1:1,000 IRDye®

680RD Goat anti-Mouse IgG (H+L) (Infrared probe labelled secondary antibody) milk suspension for ~1 h in the dark. The membranes were again washed thoroughly in TBST buffer before infrared (IR) signal quantification of associated secondary antibodies using a LI-COR ODYSSEY CLX imager was performed.

### 2.7 *Quantification of Acetate and Glycerol in Fermentation Media*

Quantification of glycerol and acetate in the cultivation media was performed by RID-HPLC. After removing samples from liquid cultures, cellular activity was immediately quenched by adding $H_2SO_4$ (final concentration: 10 mM). Particulates were removed by centrifugation at 15,000 g for 15 min, and an aliquot of the supernatant (5 µL) was loaded onto an ISERA Metab-AAC HPLC column during an isocratic run at RT with 5 mM $H_2SO_4$, 0.6 mL $min^{-1}$ as the mobile phase. Detection was done using an Agilent Refractive Index Detector (RID). The compounds were quantified by relating the RID signal to calibration curves (0.1 to 50 g $L^{-1}$) fitted with commercial standards (100,000 $RID_{13.7min}$ = 0.86 $g_{Glycerol}$ $L^{-1}$, 100,000 $RID_{15.6min}$ = 2.26 $g_{Acetate}$ $L^{-1}$).

## 3. Results

### 3.1 *Batch-mode CYP3A4 Production in Bioreactors*

To assess the effect of the DOT on CYP3A4 biosynthesis, strain JM109$^{CYP3A4/hCPR}$ was cultivated in bioreactors at different oxygen transfer rates (OTRs). Accurately maintaining constant DOTs within microaerobic ranges (and especially <10%), however, was soon found not to be technically feasible because of insufficient sensitivity and dynamics of the used oxygen probes. In order to ensure that the DOT in the individual fermentations varied only in a narrow band, we instead decided to feed $O_2$ at different constant rates. We further used predetermined $k_La^{app}$ values obtained from different aeration regimes in uninoculated reactors to categorize OTRs for different experiments, assuming that the relative differences in $k_La$ values remained similar throughout the different growth experiments. In this way, we sought to adjust different microaerobic growth regimes (*i.e.* DOT close to 0%, Table 1).

In this work, nine bioreactor experiments (**I** – **IX**) were performed (Table 1 and Table S1). Experiments **II** to **IX** were conducted at constant airflow and stirring speeds (as described above), and indeed, DOTs at or close to 0% were quickly established in experiments **III** to **IX**. Only in experiment **II**, for which we had predetermined the highest $k_La^{app}$, the DOT could still be measured with the oxygen probe and constantly remained at ~4%. This condition was hence considered microaerobic instead of late microaerobic. First, we compared functional CYP3A4 production under microaerobic (**I**; DOT = 10%, **II**; $k_La^{app}$ = 50 $h^{-1}$ ), late microaerobic (**III** – **V**; $k_La^{app}$ = 6–40 $h^{-1}$) and anaerobic (**VI**, no aeration at all) cultivation conditions and observed similar trends as measured in preliminary shake flask experiments (Figs. 1A, S2). Production of functional CYP3A4 *per* cell was low under microaerobic (**I**, **II**) and anaerobic (**VI**) conditions (black bars). As cell growth generally ceased 42 h after induction, this timepoint was henceforth applied as the maximal cultivation time, with the exception of experiment **III**, in which cells were already harvested after 30 h, because CO-binding spectra recorded from cell lysates indicated a decrease of the cellular content of functional CYP3A4 (Fig. S3). The highest concentrations of catalytically active CYP3A4 (~400 $nmol_{CYP3A4}$ $L^{-1}$) were observed at the end of the late microaerobic processes **III** (73 $nmol_{CYP3A4}$ $gCDW^{-1}$ at 5.5 gCDW $L^{-1}$) and **IV** (79 $nmol_{CYP3A4}$ $gCDW^{-1}$ at 5 gCDW $L^{-1}$). This corresponds to ~80% of the CYP3A4 yields repeatedly achieved for this strain in shake flasks in a standardized industrial setting (500 nmol $L^{-1}$).[9]

As indicated by decreasing NEN conversion rates measured for experiments **I** and **II** (Fig. S4), the highest cellular CYP3A4 activities in microaerobic conditions were most likely achieved before the first sampling point (14 h). Although CYP3A4 levels remained below the detection limit of the CO-binding assay, a western blot (WB) confirmed that functional CYP3A4 was indeed formed at early stages of experiments **I** and **II** (Fig. S5). WB also confirmed the formation of CYP3A4 below the detection limit of the CO-binding assay at anaerobic conditions. Given the WB signal intensities, we estimate volumetric yields below 260 $nmol_{CYP3A4}$ $L^{-1}$ (~40 nmol $gCDW^{-1}$ at 6.5 gCDW $L^{-1}$) at microaerobic cultivations **I** and **II**, and ~50 $nmol_{CYP3A4}$ $L^{-1}$ (48 nmol $gCDW^{-1}$ at 1.1 gCDW $L^{-1}$) for the anaerobic process **VI** (Fig. S5).

Activity measurements of CYP3A4 and *h*CPR produced in processes **I** – **VI** were performed to assess the functionality of the produced enzymes (Fig. 1A; blue and grey bars, respectively). In processes **III** – **V** the specific NEN conversion activity correlated well with the cellular amount of CYP3A4, suggesting that the formed proteins were actually converted to active enzymes (*i.e.* included an active Fe(II)-heme group). CYP3A4 turnover frequencies were relatively constant across samples drawn from the late microaerobic culture conditions (Fig. 1B).

In order to confirm sufficient stability of the enzymes over the time required for the activity assays (<30 min), we subjected *h*CPR and CYP3A4 to an enzyme stability assay, by measuring enzyme activities for extended reaction times (up to 2 h). We found that CYP3A4 activity decreased significantly after ~1 h of reaction time, whereas *h*CPR retained its activity after 2 h (Fig. S6).

Surprisingly, *h*CPR activity, in general, did not seem to be limiting CYP3A4 activity. Poor electron transport (*i.e.* because of poor coupling) from the reductases to the monooxygenase enzymes is a well-known limitation[17] but unlikely to constitute a

Table 1. Overview of tested fermentation protocols I – IX. (n.d.: not detectable; *average yields with sd, n=2*)

| ID | Aeration regime | $k_La^{app}$ [$h^{-1}$] | Mode | Cellular CYP3A4 content [$nmol_{CYP3A4}$ $gCDW^{-1}$] | CYP3A4 yield [$nmol_{CYP3A4}$ $L^{-1}$] |
|---|---|---|---|---|---|
| **I** | microaerobic (DOT 10%) | not constant | batch | n.d. | **n.d.** |
| **II** | microaerobic (DOT ~4%) | 50 | batch | n.d. | **n.d.** |
| **III** | late microaerobic | 40 | batch | 73 ± 4 | **399 ± 22** |
| **IV** | late microaerobic | 16 | batch | 79 ± 2 | **398 ±10** |
| **V** | late microaerobic | 6 | batch | 88 ± 12 | **185 ± 25** |
| **VI** | anaerobic | 0 | batch | n.d. | **n.d.** |
| **VII** | late microaerobic | 25 | batch | 72 | **396 ± 2** |
| **VIII** | late microaerobic | 8 | batch | 57 ± 2 | **110 ± 4** |
| **IX** | late microaerobic | 25 | fed-batch | 107 ± 8 | **681 ± 50** |

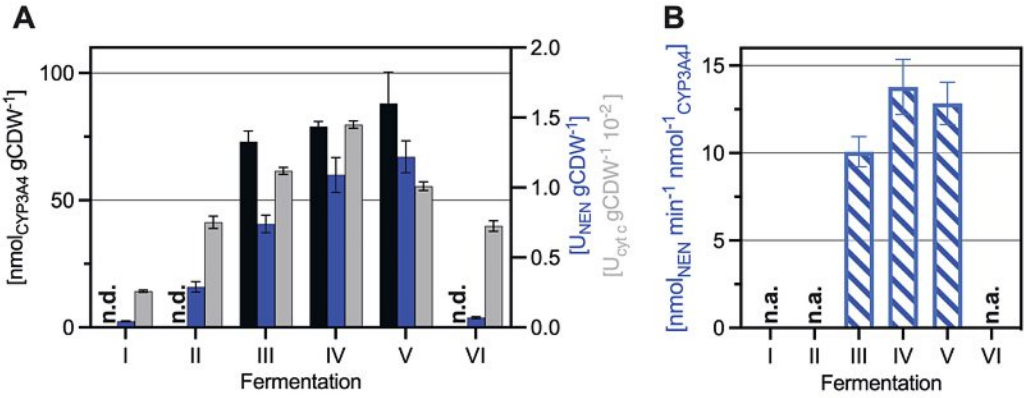


Fig. 1. Cell specific CYP3A4/hCPR production and enzyme activities in batch processes I – VI. A) All assays were performed with crude cell lysates of **JM109**$^{CYP3A4/hCPR}$ whereby CYP3A4 concentrations were determined spectrophotometrically after binding of CO to the heme-stabilized iron center (black bars), NEN conversion rates were determined by fluorometry (blue bars), and *h*CPR activity by absorbance signal of reduced cytochrome c (grey bars). B) turnover frequencies: $nmol_{NEN}$ $min^{-1}$ $nmol_{CYP3A4}^{-1}$ (activities cannot be reported for the samples without detectable CO-binding signal, since enzyme concentrations must be known for the calculation of a turnover frequency). (1 $U_{NEN}$ = 1 µmol NENH generated in 1 min, 1 $U_{cyt\ c}$ = 1 µmol cytochrome c reduced in 1 min; n.d. = not detected, n.a. = not applicable; *average with sd, n = 3*).

bottleneck for this system since *h*CPR activity in the reaction assays did not correlate with NEN turnover frequency (Fig. S7) and therefore CYP3A4 activity.

### 3.2 *Process Optimization*

The cellular concentration of functional CYP3A4 in *E. coli* grown under late microaerobic conditions (experiments **III** – **V**) stabilizes approximately five hours after the onset of the stationary phase (Fig. S3B). Depletion of nutrients could be one simple explanation for this observation. However, exploring the underlying reasons for the slowdown in productivity could deliver additional insights allowing targeted intervention to rescue enzyme biosynthesis. Therefore, using off-gas analytics ($O_2$, $CO_2$), narrower sampling intervals, and HPLC analysis monitoring glycerol and acetic acid concentrations in the medium, we wanted to gain more detailed information about the processes and their limitations. Therefore, we performed two additional batch cultivations (**VII** and **VIII**) under late microaerobic conditions in a different fermenter setup with $O_2$ and $CO_2$ off-gas analytics in place. Off-gas analytics are necessary to determine the respiratory quotient (RQ) over time.[24,30] RQ allows distinguishing processes exhibiting complete carbohydrate oxidation (RQ ~1) from processes with only partial carbon source oxidation (RQ >1), which in the context of carbohydrate metabolism may serve as an empirical distinction between aerobic and fermentative regimes, respectively. Aeration rates (stirring speed and airflow) were set such that the $k_La^{app}$ values were similar to the ones determined for experiments **II** to **V** described above. In **VII** the $k_La^{app}$ was set to 25 $h^{-1}$ and therefore lay between the two $k_La^{app}$ values of processes **III** and **IV** (40 $h^{-1}$ and 16 $h^{-1}$) with the highest volumetric product concentration. **VIII** ($k_La^{app}$ = 8 $h^{-1}$) was set to match **V** (6 $h^{-1}$) which was found to give the highest cellular content of active CYP3A4, but suffered from poor space-time yields due to slow cell growth. At a $k_La^{app}$ of 8 $h^{-1}$ (**VIII**), cell growth stopped after less than 10 h (~2 gCDW $L^{-1}$), while at a $k_La^{app}$ of 25 $h^{-1}$ (**VII**) cells kept growing for 24 h (~6 gCDW $L^{-1}$, Fig. S8A). The RQs measured for **VIII** ($k_La^{app}$ = 8 $h^{-1}$) and **VII** ($k_La^{app}$ = 25 $h^{-1}$) reached a steady state of around 2 for the former and 1 for the latter experiment, which could be an indication that the two process conditions lie in a primarily fermentative (**VIII**) and microaerobic (**VII**) range, respectively[19,31] (Fig. S8B).

As expected, the volumetric CYP3A4 yield from process **VIII** ($k_La^{app}$ = 8 $h^{-1}$) was only 108 $nmol_{CYP3A4}$ $L^{-1}$ (56.9 $nmol_{CYP3A4}$ $gCDW^{-1}$ at 1.9 gCDW $L^{-1}$). Process **VII** ($k_La^{app}$ = 25 $h^{-1}$) yielded 446 $nmol_{CYP3A4}$ $L^{-1}$ (72 $nmol_{CYP3A4}$ $gCDW^{-1}$ at 6.2 gCDW $L^{-1}$). While cells in experiment **VIII** steadily produced active CYP3A4 for the first 24 h, in **VII**, the production stopped after 18 h (Fig. S8C) coinciding with the depletion of the designated carbon source (glycerol) and peak concentrations for acetate (6.4 g $L^{-1}$). The cells then started to consume the accumulated acetate. Upon acetate depletion, a rise of DOT at 38 h indicated cell starvation which is why **VII** was terminated already at 40 h.

Under fermentative conditions (**VIII**), only about 35% of the glycerol was consumed, while acetate formation was comparable to the peak values observed in **VII** (Fig. S8D). In the most productive phase of **VII** (10–18 h after induction) glycerol was consumed at an estimated rate of 0.075 ± 0.005 $g_{Glycerol}$ $gCDW^{-1}$ $h^{-1}$ at a biomass formation rate of ~0.21 ± 0.04 gCDW $h^{-1}$. These results indicated that in the productive process **VII** additional glycerol might have allowed further cell growth and therefore CYP3A4 production. A glycerol supply strategy could hence further increase CYP3A4 space-time yields.

### 3.3 *Fed-batch Fermentation*

To test if increased glycerol availability under optimized aeration conditions (*i.e.* $k_La^{app}$ of 25 $h^{-1}$) would prolong the period of active CYP3A4 production, we designed a fed-batch run (**IX**) with two major changes compared to **VII**: First, as a glycerol feed was installed, the initial glycerol concentration could be reduced, possibly decreasing the formation of metabolites (most importantly acetate) that could impair bacterial growth. Second, spent glycerol could be replenished in order to avoid cessation of growth at an early stage.

At the time when process **IX** was started, 0.5 $g_{Glycerol}$ $L^{-1}$ were added. The cells grew and a DOT of 0% was reached after 1.5 h (Fig. S9B). However, soon thereafter, the DOT began to rise, indicating reduced oxygen consumption due to a lack of glycerol. Indeed, after re-supplying glycerol to 0.5 g $L^{-1}$ the DOT promptly decreased again and remained below the lower limit of detection for the rest of the process. At 14–16 h after induction, the cell density in **IX** (3.4 gCDW $L^{-1}$) started to fall below the one recorded in batch cultivation **VII** at the same time point (4.2 gCDW $L^{-1}$), and we started a glycerol feed at 0.070 $g_{Glycerol}$ $h^{-1}$ $gCDW^{-1}$ (details in Supplementary Information). With this feeding strategy, a cumulative amount of 7.5 g $L^{-1}$ glycerol had been added after 42 h, in contrast to the 5 g $L^{-1}$ that were added in **VII**. Positively, acetate accumulation was indeed reduced by 50% (from 6.4 g $L^{-1}$ in **VII** to ~3.5 g $L^{-1}$ in **IX**; Fig. S9D). Furthermore, the amount of func-

tional CYP3A4 increased strongly after the glycerol feed protocol had been initiated (Fig. S9E), and exceeded the levels measured in the batch process by almost 50%. The final volumetric yield in **IX** of 681 nmol $L^{-1}$ (106.9 $nmol_{CYP3A4}$ $gCDW^{-1}$ at 6.4 gCDW $L^{-1}$) also exceeded the CYP3A4 yields reported for this strain by ~36%.[9] Of note, initiation of the glycerol feed also ensured that the RQ remained constant at ~1 indicating full carbohydrate oxidation. Hence, the cells did not enter an anaerobic growth regime but continued to grow under late microaerobic conditions at essentially all times (Fig. S9F).

In process **IX**, the cellular concentrations of both CYP3A4 and *h*CPR increased over time as indicated by CO-binding, NEN-conversion, and cytochrome c reduction assays (Fig. 2A). Cellular CYP3A4 concentrations as measured by the CO-binding assay correlated well with cell-specific NEN conversion, indicating that either of the two assays allows quantification of the fraction of catalytically active CYP3A4, and that the turnover frequency of the enzyme remained relatively constant (between 11.8–14.6 $nmol_{NEN}$ $min^{-1}$ $nmol_{CYP3A4}{}^{-1}$) throughout the cultivation process (Fig. 2B).

The turnover frequency of CYP3A4 produced in fed-batch process **IX** was similar to that of the best-performing batch process **III** (13.8 ± 1.6 $nmol_{NEN}$ $min^{-1}$ $nmol_{CYP3A4}{}^{-1}$), indicating that the fed-batch protocol imposed neither negative nor positive effects on the activity of the harvested enzymes. The specific NEN conversion rates were therefore improved from 1.3 $U_{NEN}$ $gCDW^{-1}$ in initial shake flask experiments to 1.6 $U_{NEN}$ $gCDW^{-1}$ (+23%) for the final fed-batch process (**IX**).

## 4. Discussion

The aim of this work was the characterization and optimization of a process for the recombinant production of functional human cytochrome P450 CYP3A4 monooxygenase with its redox partner human cytochrome P450 reductase. Upscaling production of functional human CYP is a formidable challenge requiring rigorous molecular and process engineering efforts.[10] In this work, we specifically focused on the aspect of bioprocess optimization with an engineered CYP expression system used in the pharmaceutical industry.

In the first part, we compared three cultivation regimes: microaerobic, late microaerobic and anaerobic. For the late microaerobic conditions, the final biomass concentrations increased with increasing aeration and therefore oxygen supply rates. This suggests that cell growth is limited by the $O_2$ supply.

The CO-binding assay was not sensitive enough to allow CYP3A4 quantification under microaerobic (**I**, **II**) and anaerobic (**VI**) conditions (*i.e.* to measure enzyme concentrations below 50 nmol $gCDW^{-1}$). However, WB and enzyme activity assays clearly indicated that CYP3A4 was still produced albeit in very low quantities. Increasing the cell density in the CO-binding assay (*i.e.* $OD_{600}$ > 25) in order to adjust higher volumetric CYP3A4 concentrations was not possible, as the increasing turbidity of lysate interfered with the spectral method (results not shown). Nevertheless, if cells were grown under late microaerobic conditions, CYP3A4 could be reliably quantified by CO-binding. CO-binding data correlated well with the WB assay indicating that all (or most) of the produced CYP3A4 was catalytically active.

Growth under late microaerobic conditions proved to yield the highest cell-specific CYP3A4 concentration ($U_{NEN}$ $gCDW^{-1}$) while only negligible amounts were formed under microaerobic or anaerobic conditions. Experiments **I** – **VI** provided important clues about the cultivation conditions allowing for efficient CYP3A4 production. Because in late microaerobic fermentations, the $k_La$ is proportional to OTR, the $k_La^{app}$ values determined in the absence of cells represented a valid and useful parameter for discrimination of the oxygen feeding rates during late microaerobic growth.

In fermentations **VII** ($k_La^{app}$ = 25 $h^{-1}$) and **VIII** ($k_La^{app}$ = 8 $h^{-1}$), glycerol consumption and acetate formation profiles differed considerably. Whereas in **VIII** only ~33% of the glycerol was consumed over the whole process, it was fully depleted in **VII** already after 18–20 h. Once consumed, CYP3A4 production came to a halt and acetate concentrations peaked. These observations suggest that under these conditions (batch fermentation at $k_La^{app}$ = 8–25 $h^{-1}$), glycerol depletion and/or acetate accumulation and its subsequent consumption impairs the production of active CYP3A4. Of note, acetate concentrations comparable to the peak values measured in **VII** (~6.4 $g_{Acetate}$ $L^{-1}$) had indeed been shown to decrease the specific growth rate of *E. coli* by almost 50%.[32] Alternatively, CYP3A4 production may have discontinued if cells grew only on acetate. As acetate is a low-energy carbon source,[33] energy-intense processes such CYP3A4 production may just not be possible anymore.

This notion is also corroborated by the fact that glycerol feeding rescued CYP3A4 production in experiment **IX**. A similar observation was made by Vail *et al.* as they reported a 30% increase in the yield of the CYP3A4 varient Δ3–24 by changing from batch to glycerol fed-batch on TB (420 $nmol_{CYP3A4}$ $L^{-1}$ *vs* 320 $nmol_{CYP3A4}$ $L^{-1}$).[11] Similarly, the fed-batch process (**IX**) reported herein pro-

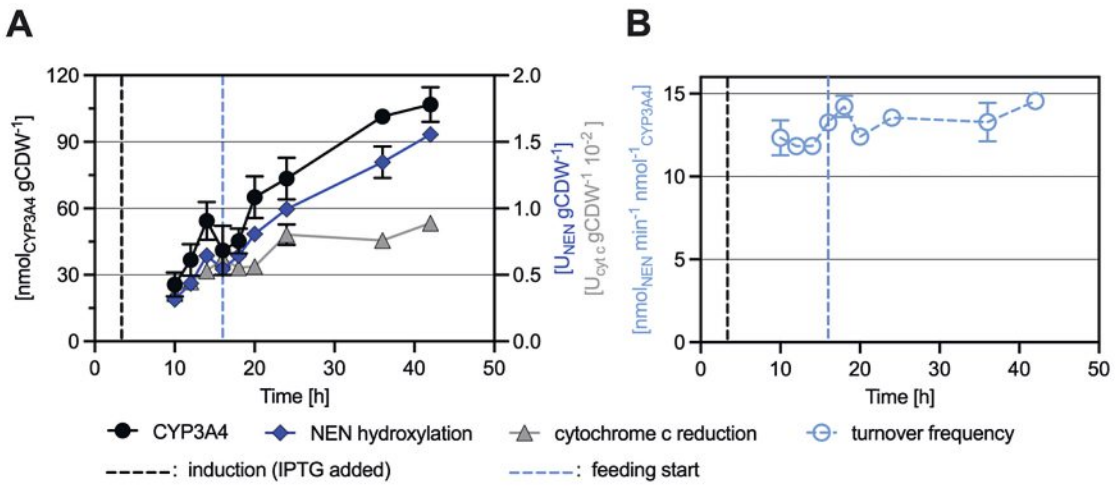


Fig. 2. Cell specific CYP3A4/*h*CPR production and enzyme activities in fed-batch process **IX** over time. A) CYP3A4 production as determined with CO-binding assay, *h*CPR activity, and NEN conversion rates per gCDW. B) NEN conversion activity per $nmol_{CYP3A4}$ (turnover frequency). Activities were measured at lysate densities corresponding to 50 nM CYP3A4 (0.2-1 $mg_{Protein}$ $mL^{-1}$). (1 $U_{NEN}$ = 1 µmol NENH generated in 1 min., 1 $U_{cyt\ c}$ = 1 µmol cytochrome c reduced in 1 min.; *average with sd, n = 3*).

duced 681 $nmol_{CYP3A4}$ $L^{-1}$, 53% more CYP3A4 than the corresponding batch-process (**VII**; 446 $nmol_{CYP3A4}$ $L^{-1}$) ($k_La^{app}$ = 25 $h^{-1}$) and ~35% more than in the original work from Pritchard *et al.* (500 $nmol_{CYP3A4}$ $L^{-1}$).[9]

Furthermore, even though in process **IX** ~50% more glycerol was supplied than in **VII**, only about half the amount of acetate (3.5 $g_{Acetete}$ $L^{-1}$) accumulated. As initially only 1.0 $g_{Glycerol}$ $L^{-1}$ was present, a considerable fraction of the acetate formed within the batch phase (**IX**) must have been produced from amino acids.[34] The sudden onset of acetate consumption before initiating glycerol feeding (≤10 h) likely indicates depletion of certain amino acids which could affect bacterial growth and therefore also protein production.[35] Further optimization experiments should also focus on the availability of amino acids. In fact, Vail *et al.* reported that varying complex media formulations (changing yeast extract brands and providing casamino acids instead of tryptone; YECA 2) allowed doubling the CYP3A4 yields in Δ3–24 in fed-batch process (from 420 $nmol_{CYP3A4}$ $L^{-1}$ in TB to 890 $nmol_{CYP3A4}$ $L^{-1}$ in YECA 2 media).[11]

Future studies on the production of CYP3A4 in fed-batch processes under late microaerobic growth conditions with YECA 2 or a specifically tailored amino acid source may hence allow to further increase CYP3A4 space-time yields. An additional approach could be careful optimization of the feeding protocol (*i.e.,* initial glycerol concentration, starting point, rate, *etc*.).

In conclusion, this work shows that, most importantly, the maintenance of fine-tuned late microaerobic growth conditions, but also the continuous supply of the energy and carbon source, and the reduction of acetate accumulation lead to elevated CYP3A4 space-time yields.

### Supplementary Information

Supplementary Information is available for this article at https://doi.org/1053/chimia.2023.417.

### Acknowledgements

We thank Dr. Stephen Hanlon and F. Hoffmann La-Roche Ltd. for providing us with the $JM109^{CYP3A4/hCPR}$ strain and for valuable input on the state of art of industrial drug metabolite synthesis. Furthermore, we thank Dr. Tsvetan Kardashliev for supporting our work with helpful advice and discussions.

Received: February 16, 2023

[1] N. T. Issa, H. Wathieu, A. Ojo, S. W. Byers, S. Dakshanamurthy, *Curr. Drug Metab*. **2017**, *18*, 556, https://doi.org/10.2174/1389200218666170316093301.
[2] S. M. Paul, D. S. Mytelka, C. T. Dunwiddie, C. C. Persinger, B. H. Munos, S. R. Lindborg, A. L. Schacht, *Nat. Rev. Drug Discov*. **2010**, *9*, 203, https://doi.org/10.1038/nrd3078.
[3] K. Schroer, M. Kittelmann, S. Lütz, *Biotechnol. Bioeng*. **2010**, *106*, 699, https://doi.org/10.1002/bit.22775.
[4] N. D. Fessner, M. Srdič, H. Weber, C. Schmid, D. Schönauer, U. Schwaneberg, A. Glieder, *Adv. Synth. Catal*. **2020**, *362*, 2725, https://doi.org/10.1002/adsc.202000251.
[5] U. M. Zanger, M. Schwab, *Pharmacol. Ther*. **2013**, *138*, 103, https://doi.org/10.1016/j.pharmthera.2012.12.007.
[6]I. F. Sevrioukova, T. L. Poulos, *Dalton Trans.* **2013**, *42*, 3116, https://doi.org/10.1039/C2DT31833D.
[7] F. P. Guengerich, Q. Cheng, *Pharmacol. Rev*. **2011**, *63*, 684, https://doi.org/10.1124/pr.110.003525.
[8] C. A. Lee, S. H. Kadwell, T. A. Kost, C. J. Serabjitsingh, *Arch. Biochem. Biophys*. **1995**, *319*, 157, https://doi.org/10.1006/abbi.1995.1278.
[9] M. P. Pritchard, R. Ossetian, D. N. Li, C. J. Henderson, B. Burchell, C. R. Wolf, T. Friedberg, *Arch. Biochem. Biophys*. **1997**, *345*, 342, https://doi.org/10.1006/abbi.1997.0265.
[10] T. Shang, C. M. Fang, C. E. Ong, Y. Pan, *BioTech* **2023**, *12*, 17, https://doi.org/10.3390/biotech12010017.
[11] R. B. Vail, M. J. Homann, I. Hanna, A. Zaks, *J. Ind. Microbiol. Biotechnol*. **2005**, *32*, 67, https://doi.org/10.1007/s10295-004-0202-1.
[12] E. M. J. Gillam, T. Baba, B. R. Kim, S. Ohmori, F. P. Guengerich, *Arch. Biochem. Biophys.* **1993**, *305*, 123, https://doi.org/10.1006/abbi.1993.1401.
[13] Y. Kanamori, K.-I. Fujita, K. Nakayama, H. Kawai, T. Kamataki, *Drug Metab. Pharmacokinet*. **200**3, *18*, 42, https://doi.org/10.2133/dmpk.18.42.
[14] F. P. Guengerich, *Annu. Rev. Pharmacol. Toxicol*. **1999**, *39*, 1, https://doi.org/10.1146/annurev.pharmtox.39.1.1.
[15] M. E. Albertolle, F. Peter Guengerich, *J. Inorg. Biochem*. **2018**, *186*, 228, https://doi.org/10.1016/j.jinorgbio.2018.05.014.
[16] D. Holtmann, F. Hollmann, *ChemBioChem* **2016**, *17*, 1391, https://doi.org/10.1002/cbic.201600176.
[17] D. Degregorio, S. D'Avino, S. Castrignanò, G. Di Nardo, S. J. Sadeghi, G. Catucci, G. Gilardi, *Front. Pharmacol*. **2017**, *8*, 1, https://doi.org/10.3389/fphar.2017.00121.
[18] K. Bettenbrock, H. Bai, M. Ederer, J. Green, K. J. Hellingwerf, M. Holcombe, S. Kunz, M. D. Rolfe, G. Sanguinetti, O. Sawodny, P. Sharma, S. Steinsiek, R. K. Poole, *Adv. Microb. Syst. Biol*. **2014**, *64*, 65, https://doi.org/10.1016/B978-0-12-800143-1.00002-6.
[19] L. Pedraz, N. Blanco-Cabra, E. Torrents, *FASEB J.* **2020**, *34*, 2912, https://doi.org/10.1096/fj.201902861R.
[20] M. W. Voice, Y. Zhang, C. R. Wolf, B. Burchell, T. Friedberg, *Arch. Biochem. Biophys*. **1999**, *366*, 116, https://doi.org/10.1006/abbi.1999.1192.
[21] C.-H. Yun, S.-K. Yim, D.-H. Kim, T. Ahn, *Curr. Drug Metab*. **2006**, *7*, 411, https://doi.org/10.2174/138920006776873472.
[22] T. H. Richardson, F. Jung, K. J. Griffin, M. Wester, J. L. Raucy, B. Kemper, L. M. Bornheim, C. Hassett, C. J. Omiecinski, E. F. Johnson, *Arch. Biochem. Biophys*. **1995**, *323*, 87, https://doi.org/10.1006/abbi.1995.0013.
[23] J. Ning, W. Wang, G. Ge, P. Chu, F. Long, Y. Yang, Y. Peng, L. Feng, X. Ma, T. D. James, *Angew. Chem. Int. Ed*. **2019**, *58*, 9959, https://doi.org/https://doi.org/10.1002/anie.201903683.
[24] C. J. Franzén, E. Albers, C. Niklasson, *Chem. Eng. Sci*. **1996**, *51*, 3391, https://doi.org/10.1016/0009-2509(95)00416-5.
[25] M. O. Cerri, M. Nordi Esperança, A. Colli Badino, M. Perencin de Arruda Ribeiro, *J. Chem. Technol. Biotechnol*. **2016**, *91*, 3061, https://doi.org/10.1002/jctb.4937.
[26] F. Gong, G. Liu, X. Zhai, J. Zhou, Z. Cai, Y. Li, *Biotechnol. Biofuels* **2015**, *8*, 86, https://doi.org/10.1186/s13068-015-0268-1.
[27] F. P. Guengerich, M. V. Martin, C. D. Sohl, Q. Cheng, *Nat. Protoc*. **2009**, *4*, 1245, https://doi.org/10.1038/nprot.2009.121.
[28] C. L. Hulse, J. M. Tiedje, B. A. Averill, *Anal. Biochem*. **1988**, *172*, 420, https://doi.org/10.1016/0003-2697(88)90464-2.
[29] U. K. Laemmli, *Nature* **1970**, *227*, 680, https://doi.org/10.1038/227680a0.
[30] V. Lyubenova, M. Ignatova, O. Roeva, S. Junne, P. Neubauer, *Processes* **2020**, *8*, 1307, https://doi.org/10.3390/pr8101307.
[31] C. Hicks Pries, A. Angert, C. Castanha, B. Hilman, M. S. Torn, *Biogeosciences* **2020**, *17*, 3045, https://doi.org/10.5194/bg-17-3045-2020.
[32] S. Pinhal, D. Ropers, J. Geiselmann, H. de Jong, *J. Bacteriol*. **2019**, *201*, e00147, https://doi.org/10.1128/JB.00147-19.
[33]R. Kutscha, S. Pflügl, *Int. J. Mol. Sci.* **2020**, *21*, 8777, https://doi.org/10.3390/ijms21228777.
[34] A. Maser, K. Peebo, R. Vilu, R. Nahku, *Res. Microbiol*. **2020**, *171*, 185, https://doi.org/10.1016/j.resmic.2020.02.001.
[35] A. Maser, K. Peebo, R. Nahku, *Microbiology* **2019**, *165*, 37, https://doi.org/10.1099/mic.0.000742.

### License and Terms